ELSEVIER

Quaternary Science Reviews 26 (2007) 2113–2127

QSR

Modelling Antarctic sea-level data to explore the possibility of a dominant Antarctic contribution to meltwater pulse IA

S.E. Bassett[a,1], G.A. Milne[a,*], M.J. Bentley[b,c], P. Huybrechts[d,e]

[a]*Department of Earth Sciences, Durham University, Science Laboratories, Durham DH1 3LE, UK*
[b]*Department of Geography, Durham University, Science Laboratories, Durham DH1 3LE, UK*
[c]*British Antarctic Survey, High Cross, Madingley Road, Cambridge CB3 0ET, UK*
[d]*Departement Geografie, Vrije Universiteit Brussel, Pleinlaan 2, B-1050 Brussel, Belgium*
[e]*Alfred-Wegener-Institut für Polar- und Meeresforschung, Postfach 120161, D-27515 Bremerhaven, Germany*

Received 25 April 2006; received in revised form 23 May 2007; accepted 17 June 2007

Abstract

We compare numerical predictions of glaciation-induced sea-level change to data from 8 locations around the Antarctic coast in order to test if the available data preclude the possibility of a dominant Antarctic contribution to meltwater pulse IA (mwp-IA). Results based on a subset of 7 spherically symmetric earth viscosity models and 6 different Antarctic deglaciation histories indicate that the sea-level data do not rule out a large Antarctic source for this event. Our preliminary analysis indicates that the Weddell Sea is the most likely source region for a large (~9 m) Antarctic contribution to mwp-IA. The Ross Sea is also plausible as a significant contributor (~5 m) from a sea-level perspective, but glacio-geological field observations are not compatible with such a large and rapid melt from this region. Our results suggest that the Lambert Glacier component of the East Antarctic ice sheet experienced significant retreat at the time of mwp-IA, but only contributed ~0.15 m (eustatic sea-level change). All of the ice models considered under-predicted the isostatic component of the sea-level response in the Antarctic Peninsula and the Sôya Coast region of the East Antarctic ice sheet, indicating that the maximum ice thickness in these regions is underestimated. It is therefore plausible that ice melt from these areas, the Antarctic Peninsula in particular, could have made a significant contribution to mwp-IA.
© 2007 Elsevier Ltd. All rights reserved.

1. Introduction

Observations of sea-level changes provide one of the primary data sets for constraining the geometry, volume and melt history of past and present glacial masses. Regions far from areas of previous glaciation (far-field sites) are sensitive to glacial meltwater influx and have therefore provided useful constraints on the temporal variation and magnitude of this influx (also known as the eustatic function) from the last glacial maximum (LGM) to the present day (e.g. Fleming et al., 1998; Okuno and Nakada, 1999; Lambeck et al., 2002; Peltier, 2002; Shennan et al., 2002). Sea-level records in regions close to areas of previous glaciation (near-field sites) are sensitive to variations in the local ice history and the associated isostatic response of the solid Earth. These observations have, therefore, been employed to infer information relating to both local ice and earth parameters and, to a lesser extent, the global meltwater influx (e.g. Tushingham and Peltier, 1991; Lambeck, 1995; Kaufmann, 1997; Mitrovica and Forte, 1997; Lambeck et al., 1998; Nakada et al., 2000; Peltier et al., 2002; Shennan et al., 2002).

Far-field sea-level observations from Barbados and the Sunda shelf (Fairbanks, 1989; Hanebuth et al., 2000) show a rapid, large-magnitude rise in sea level at around 14 calibrated kyr before present (cal kyr BP). This event, termed meltwater pulse IA (mwp-IA), is responsible for 20–25% of the eustatic sea-level rise observed from the LGM to present. Such a rapid, large-magnitude event

*Corresponding author. Tel.: +44 191 334 2332; fax: +44 191 334 2301.
E-mail address: g.a.milne@durham.ac.uk (G.A. Milne).
[1]Now at JBA Consulting, South Barn, Broughton Hall, Skipton, North Yorkshire BD23 3AE, UK.

0277-3791/$ - see front matter © 2007 Elsevier Ltd. All rights reserved.
doi:10.1016/j.quascirev.2007.06.011

would have had a significant effect on global climate and would have produced dramatically different influences on the climate system depending on the distribution of melt water sources for this event. For example, recent research has shown that a significant southern hemisphere source for mwp-IA may explain the onset of the Bølling-Allerød warm interval (Weaver et al., 2003). However, this result remains controversial given the current debate on whether the mwp-IA event was sourced primarily from the northern or southern hemispheres (Clark et al., 1996, 2002; Bassett et al., 2005; Peltier, 2005).

Recent research has shown that far-field sea-level observations can be used to constrain the source geometry as well as the magnitude of major ice melt events (Clark et al., 2002; Bassett et al., 2005). Clark et al. (2002) used the data that span mwp-IA (Barbados and Sunda shelf) to investigate the source geometry and found that the observations ruled out a dominant contribution from North American ice but were consistent with a small number of other scenarios, including that of a dominant contribution from Antarctica. Alternatively, Peltier (2005) argued that due to the lack of far-field data that capture the magnitude of mwp-IA and the difficulty associated with accurately estimating the magnitude of the rise at these two sites, the observational error permits a sole Northern Hemisphere source scenario that is dominated by the Laurentide ice sheet.

More recently, Bassett et al. (2005) extended the work of Clark et al. (2002) to consider the full viscoelastic solid earth response to mwp-IA. This extension permits the use of sea-level observations from Tahiti and the Huon Peninsula which capture the sea-level response following mwp-IA. By modelling this extended data set, Bassett et al. (2005) concluded that a dominant Antarctic contribution to mwp-IA (~15 m eustatic equivalent) is required to fit the far-field observations with a single ice history and earth model.

Results from ocean circulation modelling also support the scenario of a dominant southern hemisphere contribution to mwp-IA. For example, Manabe and Stouffer (1997) showed that a large North American source to the Atlantic Ocean has been shown to cause a considerable cooling of the northern hemisphere which is not observed in the proxy records (McManus et al., 2004). Weaver et al. (2003) demonstrated, on the other hand, that a large influx from the Antarctic would cause a strengthening of North Atlantic deepwater formation and a consequent warming of the North Atlantic region. Such a scenario is therefore a plausible mechanism to explain the onset of the Bølling Allerød warm interval, and subsequently, through freshwater forcing from the Laurentide and Fennoscandian ice sheets, the Younger Dryas cold period (Weaver et al., 2003). A 15 m southern source scenario is also in keeping with findings from oxygen isotope modelling (Rohling et al., 2004) which show that simulations of marine oxygen isotope distributions for a number of different source scenarios compared to data from sediment cores suggest equal contributions from Antarctic and Northern ice sheets of around 15 m.

A dominant Antarctic contribution to mwp-IA must be consistent with observations and modelling that relate to the deglaciation history of the Antarctic ice sheet. The volume of ice in the Antarctic ice sheet at the LGM and the subsequent melt history has been discussed extensively in the literature (e.g. summarized in Bentley, 1999; Anderson et al., 2002). Models of the Antarctic ice sheet from glaciological, glacio-isostatic and geological reconstructions have suggested contributions to the total eustatic sea-level rise of between 1 and 38 m from LGM to present (e.g. Nakada and Lambeck, 1988; Tushingham and Peltier, 1991; Colhoun et al., 1992; Bentley, 1999; Nakada et al., 2000; Denton and Hughes, 2002; Huybrechts, 2002; Ivins and James, 2005), with more recent research favouring a narrower range of 13–21 m (e.g. Bentley, 1999; Denton and Hughes, 2002; Huybrechts, 2002).

With regard to the Antarctic deglaciation history, several recent studies suggest that the East and West Antarctic components did not advance and retreat at the same time (e.g. Bentley, 1999; Nakada et al., 2000; Anderson et al., 2002). Results from Antarctic model reconstructions suggest that the major phase of Antarctic deglaciation occurred during the Holocene (e.g. Tushingham and Peltier, 1991; Nakada et al., 2000; Huybrechts, 2002). Reconstructions from geological data suggest, however, that this may have occurred earlier, beginning at around 15 cal kyr BP, especially in the Antarctic Peninsula (e.g. Bentley, 1999; Anderson et al., 2002). It is important to note, however, that none of these studies considered the possibility of a large contribution from Antarctica to mwp-IA.

The East Antarctic ice sheet (Fig. 1) is, primarily, a land-based ice sheet bounded by the Transantarctic Mountains and a steep continental slope and is thought to have made a relatively minor contribution to post-LGM eustatic sea-level change (e.g. Bentley, 1999; Huybrechts, 2002). There are components of the East Antarctic ice sheet that had a more active grounding line, such as the Lambert Glacier region, which could have made a non-negligible contribution to mwp-IA. This suggestion is supported by field evidence from this region that indicates a rapid ice retreat between 15,370 and 13,440 cal yr BP (Verleyen et al., 2005). In contrast, the West Antarctic ice sheet is primarily marine-based and so can respond quickly to changing climate or sea levels. Most of the mass lost from Antarctica following the LGM was sourced from the West Antarctic Ice Sheet and the Antarctic Peninsula (e.g. Bentley, 1999; Huybrechts, 2002).

Of the four components of the West Antarctic ice sheet (Fig. 1), the Ross and Weddell components are believed to have lost the most mass since the LGM and so are most likely to be the primary mwp-IA source regions. The examination of glacio-geological data in the Ross Sea suggests a gradual ice retreat largely during the Holocene, with little indication of a significant contribution (>1 m)

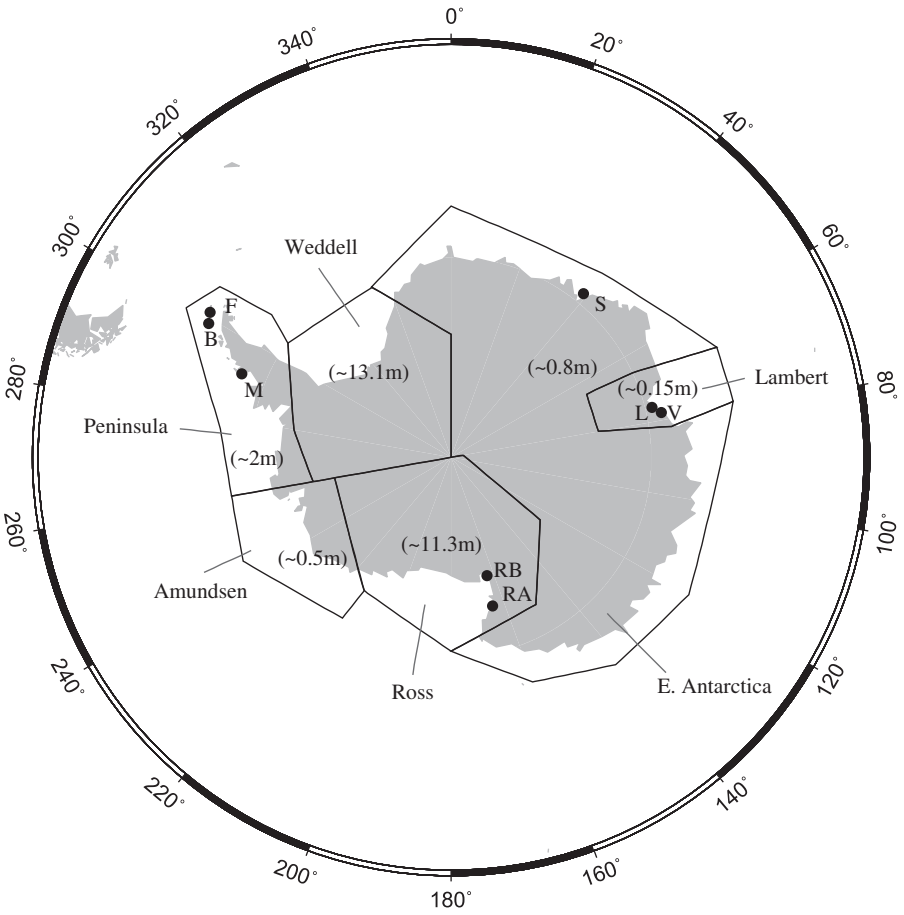

Fig. 1. Location map for data sites used in this study. These are labelled as follows. F = Fildes, B = Byers, M = Marguerite Bay, S = Sôya, L = Larsemann, V = Vestfold, RA = Ross A and RB = Ross B. This map also indicates and labels the different regions of the Antarctic ice sheet referred to in the text. Each region is also labelled with the maximum eustatic sea-level contribution contained in the model. Note that the maximum ice extent within the regions shown did not necessarily occur in a synchronous fashion or at the time of the last glacial maximum.

to mwp-IA (Conway et al., 1999; Licht, 2004). Glacio-geological data constraining the volume and melt history of the Weddell Sea region remain inconclusive (e.g. Bentley and Anderson, 1998; Anderson et al., 2002).

In this study, our main aim is to determine whether the available Antarctic near-field sea-level data preclude the possibility of a significant Antarctic contribution to mwp-IA. If we find that this is not the case, a secondary aim is to determine whether the data can be used to infer which components of the ice sheet were the most likely contributors to mwp-IA. In Section 2 we briefly review the sea-level data we employ in the modelling analysis and in Section 3 we consider the ability of the data to test the veracity of a number of different deglaciation scenarios and earth model parameters.

2. Observational data

The sea-level data sets we consider are from eight locations on the Antarctic continent (Fig. 1) and cover the period 12-0 cal kyr BP. The data are from the Antarctic Glaciological Geological Database (Hindmarsh—http://www.antarctica.ac.uk/met/rcah/agdb/index.htm) along with a number of additional, more recently published results not within the database. The model predictions are generated in cal kyr BP and so radiocarbon dates have been converted to calibrated dates using the CALIB 5.0.1 programmme (Stuiver and Reimer, 1993). Marine samples were calibrated using the Marine04 calibration curve (Hughen et al., 2004); calibration of freshwater samples used the Intcal04 curve (Reimer et al., 2004). The various data sets are described in detail below and illustrated in Fig. 2.

The sea-level reconstructions have been derived from radiocarbon dating of organic material in raised beaches (penguin guano and remains, shells, seaweed, seal skin), and in isolation basins. Isolation basins are coastal inlets or basins that become cut off from the sea as relative sea-level (RSL) falls, or are flooded by seawater as RSL rises. If these basins have freshwater input, the sedimentary record will show a change from marine to lacustrine environments for RSL fall; the reverse occurs during RSL rise. Dating the transition from marine to lacustrine sediments and measuring the height of the sill that formerly connected the lake to the ocean enables an accurate determination of mean sea-level at the time the basin became isolated. The vertical error associated with determining sill heights

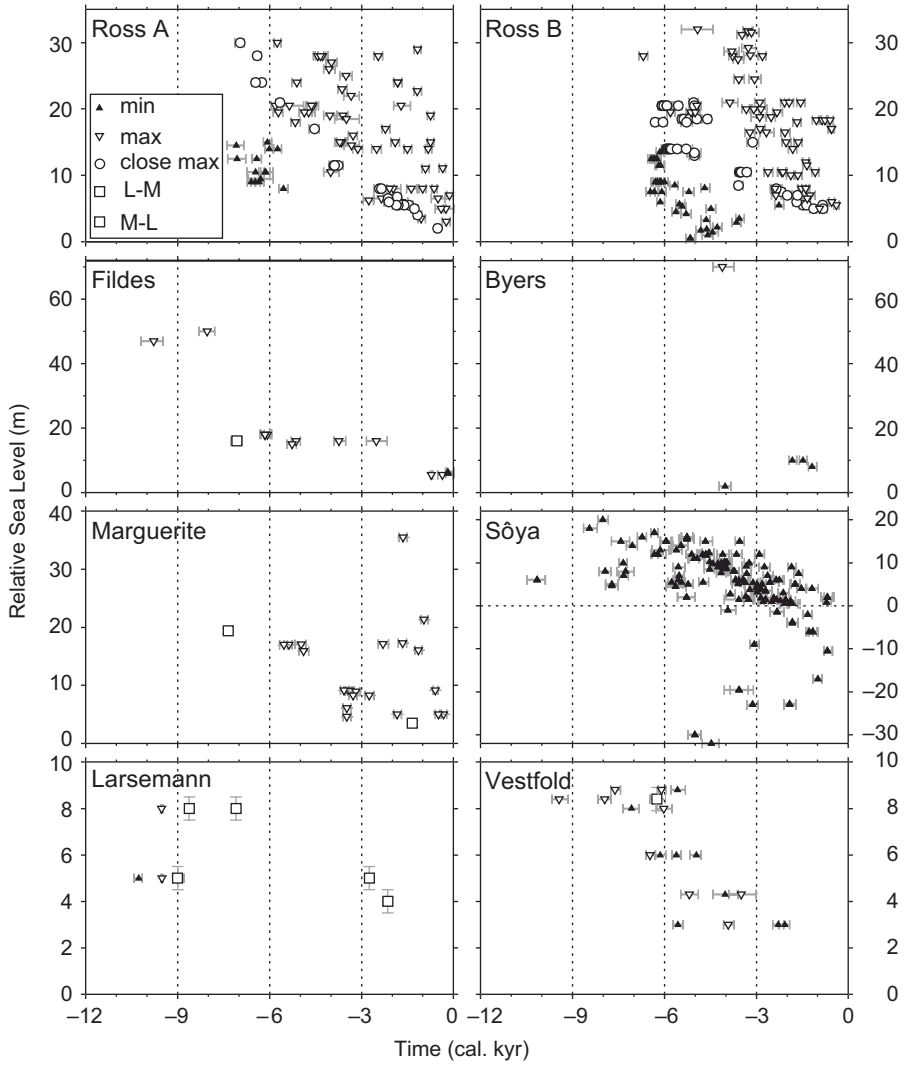

Fig. 2. Sea-level observations at the eight sites shown in Fig. 1 and discussed in detail in Section 2. The key in the Ross A frame identifies the type of sea-level constraint for a given symbol (see main text for more information). Isolation basin indicators are labelled as either lacustrine to marine (L–M) or marine to lacustrine (M–L).

relative to mean sea level are usually in the range 0.2–0.5 m (Bentley et al., 2005; Verleyen et al., 2005). We adopt a conservative height error of 0.5 m for index points derived from isolation basins.

Whilst isolation basins provide a 'fix' for sea level, all other sample types provide either minimum or maximum limits on past sea level (indicated, respectively, as black triangles and open inverted triangles in Fig. 2). For example, past sea level is interpreted to have been above shells such as *Laternula elliptica* and *Adamussium colbecki* found in situ within marine sediment and so they are interpreted as minimum sea level constraints. Both of the species used are found at a range of depths today, with a minimum habitation depth of 1–2 m. We therefore assume that past mean sea level must have been *at least* 1–2 m above the depth that a given shell was retrieved from.

Maximum sea-level constraints come from seal hairs, penguin guano and remains in ornithogenic soils and wind blown deposits resting on top of marine deposits, as well as freshwater sediments in isolation basins. All of these are interpreted to have been deposited above sea level. Given that modern storm beaches can reach a few metres above mean sea level in Antarctica (Kirk, 1991; Hall and Denton, 1999), we interpret these indicators as defining a height *at least* ~2 m above past mean sea level. Note that we have not made any account of the fact that the height of storm beach formation can vary according to the local wave climate, both along a coastline and through time.

At the two Ross Sea sites Baroni and Hall (2004) and Hall et al. (2004) report several samples of organic material (bones, shells, seal skin) that were incorporated *within* storm beaches, rather than resting on them. We follow these authors in interpreting such material as providing *close* ages for the raised beaches (i.e. they are found only a few metres above the height of past mean sea level). These data (shown as open circles in Fig. 2) can be regarded as

providing a constraint on sea-level that is intermediate in accuracy between those derived from isolation basins and those maxima for sea-level from material deposited on top of raised beaches.

For consistency we have corrected all dates from marine material for a reservoir effect of 1300 ± 100 yr (Gordon and Harkness, 1992; Berkman and Forman, 1996). The errors in the plotted dates of the index points are derived from radiocarbon analyses, the uncertainty in the marine reservoir, and the calibration of these data. Error propagation incorporates errors at the 1-sigma level throughout.

The data for the Ross Sea have been obtained from the Terra Nova Bay (Ross A in Fig. 2) and Southern Victoria Land Coast (Ross B in Fig. 2) regions of the Ross Sea (Baroni and Hall, 2004; Hall et al., 2004). Most sea level data here derive from penguin remains (maxima), shells (minima) and seal skin (close ages). These two data sets comprise, arguably, the best-constrained RSL data in Antarctica. (Hall and Denton, 1999; Baroni and Hall, 2004).

The data from the South Shetland Islands have been split into two groups to account for the spatial variation in the sea-level predictions that occurs across this region: Fildes Peninsula (King George Island) and Byers Peninsula (Livingston Island) (Fig. 1). The data are from organic remains (e.g. penguin, whale and seal bones) that provide sea-level maxima and from isolation basins which provide accurate height constraints on past sea levels (Bentley et al., 2005, and references therein).

Marguerite Bay sea-level index points were determined from isolation basins on Horseshoe Island (Wassell and Håkansson, 1992) and Pourquoi Pas Island (Bentley et al., 2005). Dates from penguin remains and guano provide maximum constraints on sea-level (Emslie and McDaniel, 2002; Bentley et al., 2005).

The data from the Sôya coast are exclusively derived from marine shells which provide sea-level minima. The data plotted here come from a series of Japanese expeditions to the Lützow-Holm Bay region of Enderby Land, and are from the youngest (Holocene) group within a set of several hundred ages ranging up to $>40\ ^{14}$C ka. Given some widely known but poorly understood problems with radiocarbon dating of marine fossils (Gordon and Harkness, 1992; Berkman and Forman, 1996) there have been some independent tests of these shell dates using Electron Spin Resonance (Takada et al., 2003). These have shown that some of the radiocarbon ages for shells may be problematic although it is not clear if this problem applies equally to the younger (Holocene) dates as it does to the older dates in the Sôya region.

The data points from the Larsemann Hills are derived from three isolation basins in the Lambert Glacier-Amery Ice Shelf system (Verleyen et al., 2005). Although geographically close to the Larsemann Hills, the sea-level observations from the Vestfold Hills are significantly displaced to those obtained from the Larsemann Hills area and so have been plotted on a separate sea-level curve for the purpose of this study. The data are from sediment cores from isolation basins (Zwartz et al., 1998) and sea-level minima are provided by shells found *in situ* within marine sediments (Zhang and Peterson, 1984).

3. Modelling

Sea-level predictions are computed by solving the revised sea-level equation described in Milne (1998) and Milne et al. (1999). Recent advances in sea-level modelling, such as perturbations to the rotation vector, time-varying shorelines, and an accurate treatment of sea-level change in regions of ablating marine-based ice are therefore incorporated in the predictions described below. The two variable inputs to the sea-level algorithm are the earth and the ice history models.

The solid earth isostatic component of the sea-level signal is computed using the impulse response formalism (Peltier, 1974) which yields the response of a spherically symmetric, self-gravitating and compressible Maxwell viscoelastic earth model to an impulse forcing. The radial elastic and density structure of the earth model is based on the seismically inferred PREM (Dziewonski and Anderson, 1981) and is depth parameterized (by volume averaging) into 25 km thick shells. The radial viscosity structure is more crudely parameterized into an upper region of effectively infinite viscosity to simulate an elastic lithosphere, and two deeper regions, each with a uniform viscosity, that correspond to the sub-lithospheric upper mantle and the lower mantle (below 670 km). These three parameters are varied in the modelling analysis. It is convenient to define a preferred, or reference, viscosity model. For this purpose we chose a 96 km thick elastic lithosphere and viscosities of 0.5×10^{21} Pa s for the upper mantle and 10^{22} Pa s for the lower mantle region. These parameters are broadly consistent with the results of a number of recent viscosity inferences (Nakada and Lambeck, 1989; Lambeck and Nakada, 1990; Lambeck et al., 1990; Lambeck, 1993; Forte and Mitrovica, 1996; Mitrovica and Forte, 1997; Lambeck et al., 1998; Milne et al., 2001).

3.1. Input ice histories

The ice histories utilized in this study were derived by combining a northern hemisphere model based on the ICE-3G reconstruction (Tushingham and Peltier, 1991; Bassett et al 2005) with a model of Antarctic ice sheet evolution output from a realistic, thermomechanical glaciological model (Huybrechts, 2002). As described below, these two components of our ice model were altered in order to test a range of mwp-IA source geometries. For each combination considered, the North American component of the northern hemisphere model was modified to provide a good fit to the Barbados sea-level record in order to ensure that the eustatic component of the hybrid ice model was accurate (Bassett et al., 2005).

The Antarctic component of our global model was adapted from a glaciological simulation using the three-dimensional thermomechanical model developed by Huybrechts (2002). The simulation, which was run on a high-resolution (20 km) grid, computes the evolution of the Antarctic ice sheet in response to a series of forcing factors, including sea level, surface temperature, snow accumulation and ice ablation below ice shelves. As described below, we alter the original simulation to examine a small range of mwp-IA source scenarios. In the original simulation, the maximum extent of the Antarctic ice sheet is attained around 10 cal kyr BP and the primary component of deglaciation occurs relatively late: between 6 and 4 cal kyr BP contributing ~17 m to eustatic sea level. This total contribution is comprised of ~7.2 m from the Ross Sea region, ~9.3 m from Weddell Sea, ~0.3 m from the Peninsula, ~0.15 m from each of the Lambert Glacier and Amundsen Sea regions. The contribution of this model to post-LGM eustatic sea-level rise is ~22 m, which is near the maximum obtained in the suite of simulations discussed in Huybrechts (2002).

3.2. Sensitivity of predictions to Antarctic versus North American source

In order to test the hypothesis of an early and rapid deglaciation of the Antarctic ice sheet, we compare predictions based on two end member mwp-IA source scenarios to the sea-level observations described in Section 2. One scenario assumes that the mwp-IA event was sourced entirely from the northern hemisphere and primarily from the North American ice complex. In order to fit the Barbados record, it was necessary to revise the Antarctic component of our ice model so that the primary component of deglaciation occurred at the same rate as in the original simulation but 4 kyr earlier (i.e. between 10 and 8 cal kyr BP).

The second scenario assumes a dominant contribution from the Antarctic ice sheet to mwp-IA. In this case, we advanced the main period of Antarctic deglaciation by 8.5 kyr compared to the original simulation and increased the rate of this event to provide ~17 m of eustatic sea-level contribution from the Antarctic between 14.5 and 13.5 cal kyr BP, with ~4 m eustatic sea-level delivered post-mwp-IA. This magnitude of mwp-IA contribution is compatible with the value of 15 m inferred from observations of far-field sea-level changes during the Lateglacial period (Bassett et al., 2005). The sea-level predictions associated with these two contrasting mwp-IA scenarios coupled to the reference earth model are shown on Fig. 3. Note that predictions are shown only for the past 12 kyr since none of the data predate this time.

In order to understand the predictions it is helpful to refer to 6 distinct regions of the Antarctic ice complex: Weddell Sea, East Antarctic, Lambert Glacier, Ross Sea, Amundsen Sea and the Antarctic Peninsula (Fig. 1). At each data site, the predicted sea-level changes will show most sensitivity to local variations in the ice model; for example, the Ross sites will be very sensitive to any change in the Ross ice sheet deglaciation. In our ice model, the Ross Sea and the Weddell Sea components are the largest contributors to the Antarctic portion of eustatic sea-level change and so sites close to these regions should exhibit the greatest sensitivity to the contrasting source scenarios described above.

Most regions show a significant change in the predictions depending on whether a North American (dashed line) or Antarctic (solid line) dominant source for mwp-IA is considered. In both sets of predictions there is a distinct change in the form of the curves at 6 cal kyr BP. This is exhibited either as a highstand (e.g. the solid black line at Marguerite, Larsemann and Vestfold) or as a change in gradient or leveling off (e.g. Fildes and Byers). This is a result of the dramatic decrease in the rate of northern hemisphere ice melt in the adopted ice model at this time.

In the dominant Antarctic source model the Ross Sea deglaciates earlier and more rapidly than in the northern hemisphere source model. At the Ross Sea sites, there is a sea-level rise associated with the northern hemisphere melting until this region deglaciates, after which there is a sea-level fall resulting from the isostatic uplift. The combined effect of these two processes is a sea-level highstand, which occurs earlier in the Antarctic source model (around 15 cal kyr BP) and thus results in a shallower sea-level fall for this model during the mid-to-late Holocene. The shallower sea-level fall predicted by this model is more consistent with the data than the larger and steeper fall predicted by the northern hemisphere source model. At the Ross A site, the Antarctic source model shows a distinct sea-level rise at 11–10 cal kyr BP. This corresponds to an increase in the eustatic component of the North American ice history in order to fit the Barbados record.

There is little difference between the two predictions at the Fildes and Byers sites after 6 cal kyr BP. The difference in the predictions prior to this time is primarily associated with ice melt in the Peninsula region. In the Antarctic source model this occurs around the time of the pulse which results in a small sea-level fall around 14 cal kyr BP associated with the isostatic uplift of the region. In the North American source model this occurs much later, around 10 cal kyr BP, and is illustrated by the deflection in the dashed line at these sites. The effect is much less noticeable in the North American model due to the unloading occurring over a longer time and during a period of more rapid eustatic rise. Both sets of model predictions for the South Shetland Islands data (Fildes and Byers) fail to match the Holocene sea-level trend indicated by the observations, which suggests that the modelled ice unloading in this area is insufficient.

The Marguerite Bay predictions reflect the proximity of this site to both the Antarctic Peninsula and Weddell Sea ice masses. The model predictions are vastly different prior to 8 cal kyr BP. In the northern hemisphere source model,

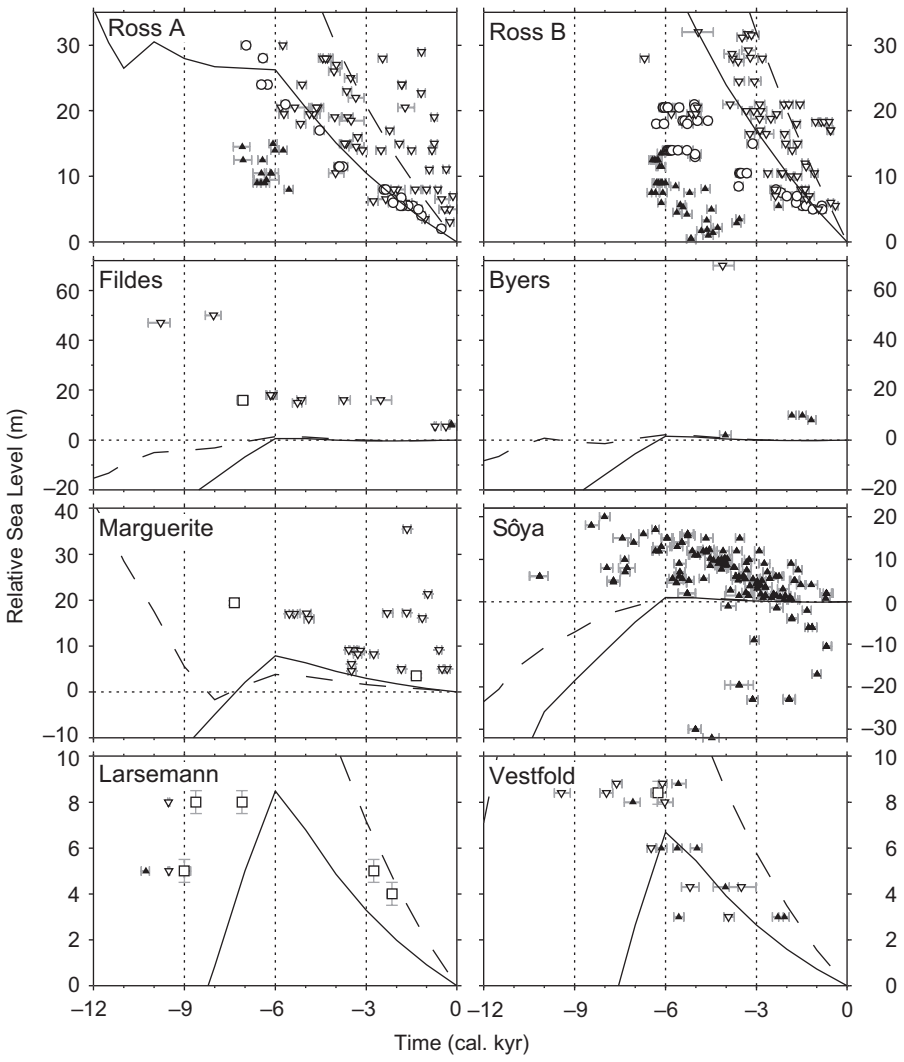

Fig. 3. Sea-level predictions based on the reference earth model and two end member mwp-IA source scenarios: a sole northern hemisphere contribution (26 m North American ice and 2 m from other sources; dashed line) and a dominant Antarctic contribution (17 m from Antarctic ice, 2 m from North American ice and 2 m from other sources; solid line). Both scenarios were tuned to fit the Barbados sea-level record. The difference in the total eustatic contribution for each scenario is a result of the distinct spatial variation, or sea-level "fingerprint", associated with model (Clark et al., 2002).

the Peninsula and Weddell Sea regions begin to deglaciate around 12 and 10 cal kyr BP, respectively. The result of this is an extended fall in sea-level, from 12 to 8 cal kyr BP, following a rise associated with northern hemisphere melting. In the Antarctic source model, this period of sea-level fall is earlier (subsequent to the mwp-IA event) and so the rate of uplift reduces significantly by around 10 cal kyr BP, leading to a eustatic-dominated sea-level rise during the early Holocene. Both models considered under-predict sea level by ~20 m around 7.5 cal kyr BP at Marguerite.

The Sôya Coast data indicate that sea level should fall at this site for the past 7 kyr from around 20 m. This is clearly not captured by either model prediction. In both of the adopted source models, there is relatively little ice volume change in the East Antarctic and so the dominant component of the signal at this site is the eustatic sea-level rise. The difference between the two predictions is predominantly related to the difference in the eustatic sea-level curves between the two ice models.

Although only a small contributor to the eustatic sea-level signal, the timing of deglaciation in the Lambert glacier region has a dramatic effect on the sea-level predictions at Larsemann and Vestfold. In the northern source model, this occurs at ~10 cal kyr BP and results in a sea-level highstand (around 25–30 m) at this time. This highstand marks the transition from a eustatic-dominated sea-level rise to an isostatic-dominated (local) sea-level fall. In the Antarctic source model, most of this region deglaciates at the time of mwp-IA and so pushes the isostatic-induced sea-level fall much earlier. The isostatic component of the signal has sufficiently relaxed by ~10 cal kyr BP so that the eustatic rise dominates the predicted signal until the cessation of rapid melting in our northern hemisphere ice model. The Antarctic source model is more compatible with the observations from

Larsemann and Vestfold, which require sea level to be rising during the early Holocene and falling by ~7 cal k-yr BP. This early Holocene rise and fall of sea level is not captured in the northern hemisphere source model.

Based on these preliminary comparisons, the Antarctic source model is more compatible with the observations at sites Ross (A & B), Larseman and Vestfold, while neither model provides a reasonable match to the observations at the remaining sites. In the following section, we extend the above results to consider the sensitivity of the predictions to plausible variations in the lithospheric thickness and viscosity structure of the adopted earth model. Such an analysis will enable us to determine if the misfit at each site for a given ice model can be accommodated by viscosity uncertainty in the adopted earth model.

3.3. Sensitivity of predictions to Earth viscosity structure

For each earth viscosity model considered, the North American ice history was scaled to maintain an accurate fit to the Barbados sea-level history. We considered the following parameter ranges in Fig. 4: lithospheric thickness (71–120 km) (Fig. 4a), upper mantle viscosity ($1-10\times10^{20}$ Pa s) (Fig. 4b) and lower mantle viscosity ($1-40\times10^{21}$ Pa s) (Fig. 4c). These specific parameter ranges were chosen to broadly encompass the results from a number of recent inferences of earth viscosity structure in different regions from GIA analyses.

Of the eight sites considered, the predictions at Fildes, Byers and Sôya are least sensitive to variations in the viscosity structure. This is directly related to the adopted ice model, which exhibits relatively little deglaciation at

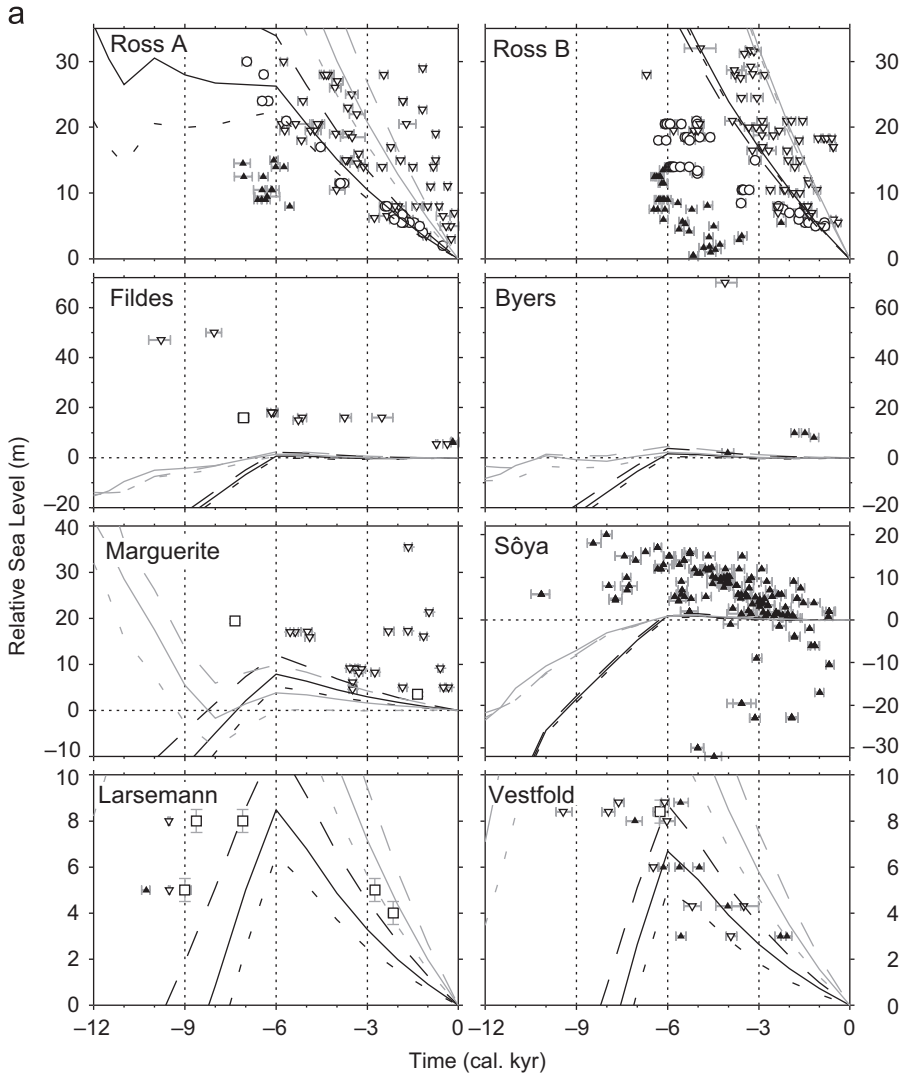

Fig. 4. (a) Sea-level predictions based on the sole northern hemisphere (gray lines) and dominant Antarctic (black lines) mwp-IA scenarios shown in Fig. 3 for the reference earth model (solid line) and two other earth models that are the same as the reference earth model except that the lithospheric thickness is increased to 120 km (dotted line) or decreased to 71 km (dashed line). (b) The same as Fig. 4a except that the upper mantle viscosity is increased to 10^{21} Pa s (dotted line) or decreased to 10^{20} Pa s (dashed line) relative to the reference model (solid line). (c) The same as Fig. 4a except that the lower mantle viscosity is increased to 4×10^{22} Pa s (dotted line) or decreased to 10^{21} Pa s (dashed line) compared to the reference model (solid line).

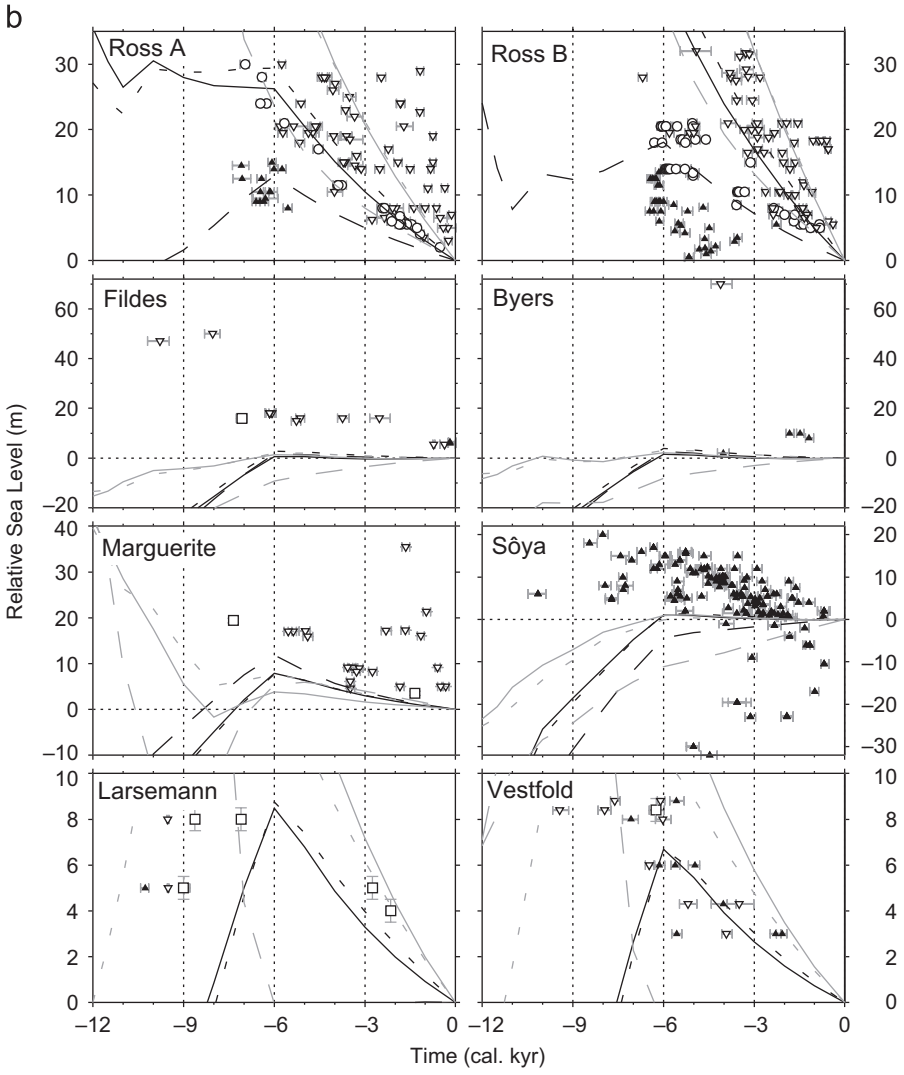

Fig. 4. (*Continued*)

these localities. The increased sensitivity at these sites to variations in deeper structure (as opposed to lithospheric thickness variations) is driven by ice sheet loading changes in other regions. In contrast, the greatest sensitivity is found at the remaining five sites which are in close proximity to components of the ice model that show larger changes during deglaciation. For these five sites (of which four were fit best by the Antarctic source model when adopting the reference earth model) it is important to ascertain if this ice model is also preferred when the sensitivity of the predictions to viscosity structure is considered.

Of the two sites in the Ross Sea region, Ross A exhibits the greatest sensitivity to variations in earth model structure. At this site, the predictions based on the Antarctic source model (black lines) envelop the observations better than those for the northern hemisphere source model (gray lines). However, the predictions based on the latter suggest that an earth model with parameter values within the ranges described above could fit the data (for example, the model with an upper mantle viscosity of 10^{20} Pa s provides a relatively good fit). At the Ross B site, the reduced sensitivity to earth structure suggests that it is not possible to fit the data for the range of earth model parameters considered. In comparison, a relatively good fit can be obtained with the Antarctic source model when values for upper and lower mantle viscosity are chosen from the lower end of the spectrum given above (e.g. 10^{20} and 10^{21} Pa s, respectively).

Predictions at the sites Larsemann and Vestfold are relatively insensitive to the range of lower mantle viscosity values considered in Fig. 4c. This indicates that the spatial scale of the ice sheet changes in this region are not large enough to induce any significant deformation within the model lower mantle. In contrast, there is a considerable sensitivity to changes in shallower earth structure (particularly upper mantle viscosity; Fig. 4b). This is only apparent for the northern hemisphere source model due to the time and height range illustrated. For the Antarctic source model, the rapidity of the solid earth

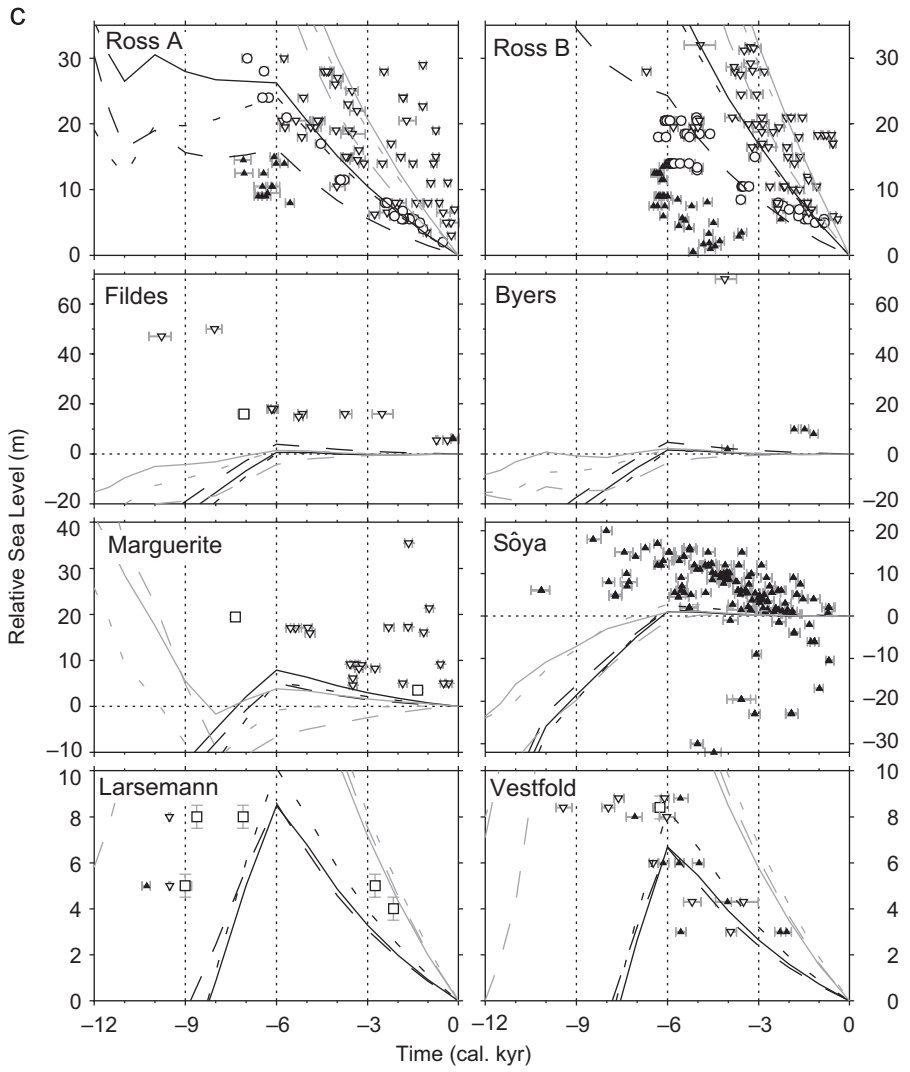

Fig. 4. (*Continued*)

response using the lowest value of upper mantle viscosity considered results in the predictions remaining below present day sea level for the entire period shown in Fig. 4b. Inspection of Fig. 4a–c indicates that the predictions based on the northern hemisphere source model do not even approach a good fit to the data and so we conclude that a rapid deglaciation of this region at the time of mwp-IA is clearly preferred at these two sites.

Regardless of the adopted earth model or ice model, the quality of data-model fit at the sites Fildes, Byers, Marguerite (index point at ~7 cal kyr BP in particular) and Sôya remain poor. This is further evidence to suggest that the adopted Antarctic ice model underestimates the maximum ice volume in these regions.

The results of this section show that: (i) while neither of the two ice models can produce an acceptable fit at all sites, the Antarctic source model is clearly preferred by data from Ross B, Larsemann and Vestfold; (ii) the data from Ross A can be fit by either ice model given a suitable earth model (with plausible parameter values); (iii) data from Fildes, Byers, Marguerite and Soyâ cannot be fit by any of the earth-ice models considered. Given that the Antarctic source model is the more successful of the two ice models considered, in the next section we explore the viability of this model further by testing the sensitivity of the predictions to changing the geometry of melt within the Antarctic ice complex at the time of mwp-IA. This additional sensitivity test will enable us to determine whether it is possible to improve the fit further and potentially constrain the source geometry at a regional scale using the available observations.

3.4. Sensitivity of predictions to geometry of Antarctic source

There are two components within our adopted Antarctic model which contain sufficient volume to contribute significantly to mwp-IA: the Ross Sea and Weddell Sea. The eustatic contributions from different regions of the ice model are shown in Fig. 1. These values correspond to the

eustatic sea-level contribution associated with the maximum glacial extent of each region considered in the Figure, which, for most regions, does not coincide with the ice extent at the time of the global glacial maximum (~20 cal kyr BP).

The Ross Sea and Weddell Sea components of the ice model contain, respectively, ~11 and ~13 m of eustatic sea level. We have tested three different mwp-IA scenarios for this preliminary study: a sole Ross or Weddell source and a combined Ross and Weddell source (~5 and ~9 m, respectively). All of the predictions shown are based on the reference earth viscosity model, which provided (overall) the best fits to the data for the dominant Antarctic source model. The results of these computations are shown in Fig. 5. As discussed above, for each ice model considered, the volume of North American ice was altered to ensure that a good fit was maintained at Barbados. Although a large Ross component to mwp-IA has been argued against on the basis of geological evidence (e.g. Licht, 2004), it has been included here to be compatible with the model adopted in the previous two sections and to make our sensitivity analysis more complete.

As expected, the sole Ross Sea model significantly alters the predictions at Ross A and Ross B. There is however little difference between the scenario in which the Ross Sea is the main contributor (dashed line) compared to that in which it is only a partial contributor (solid line), indicating that the predictions are relatively unaffected by the activity in the Weddell Sea for this time period. In both models that consider a proportion of Ross ice melt, the isostatic uplift occurs sufficiently early to result in a shallower sea-level fall compared to the predictions based on the northern hemisphere source model (see Fig. 3), in which this region deglaciates much later (10–8 cal kyr BP). The Weddell Sea model produces a fit which is similar to our northern hemisphere source model, indicating that the predicted sea-level response in the Ross Sea region is relatively insensitive to the timing and magnitude of deglaciation in the Weddell Sea. These results for the Ross Sea region

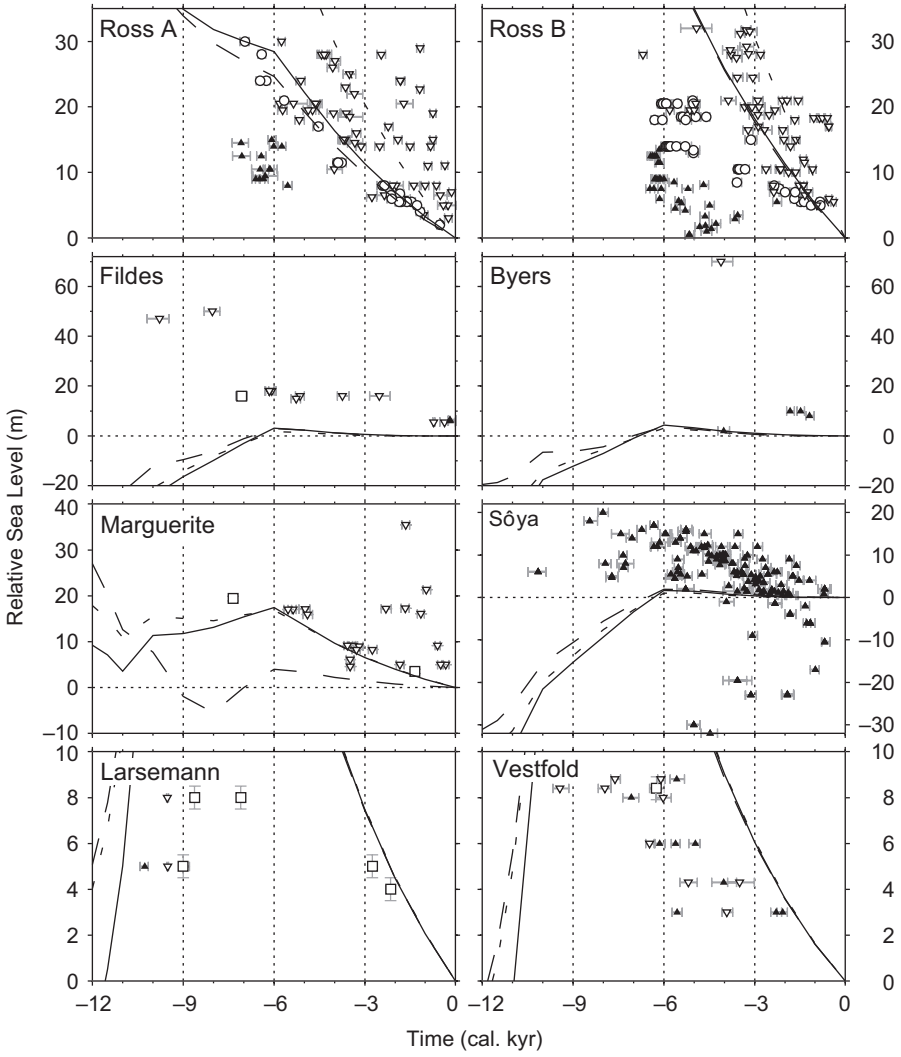

Fig. 5. Sea-level predictions based on the reference earth model and three different models of Antarctic mwp-IA melt scenarios: Ross Sea source (dashed line), Weddell Sea source (dotted line), combination of Weddell Sea and Ross Sea (solid line). See main text for more details.

suggest that: (i) either the adopted Antarctic ice model overestimates the ice volume in this region (particularly Ross B); (ii) that this region must have deglaciated early (as in the Antarctic source model) or (iii) a combination of (i) and (ii).

The Marguerite Bay observations clearly prefer the scenarios that include either a dominant or partial Weddell contribution to mwp-IA. The Ross Sea dominant scenario falls significantly below the data as a result of a large sea-level fall caused by the relatively late deglaciation of the Peninsula and the Weddell Sea in this model. In the Weddell Sea models, this sea-level fall is predicted earlier and occurs concurrently with the rapid rise in the eustatic signal. The net effect is to push the predictions higher in the Holocene, which is more consistent with the observations. Although a reasonable fit is found to the more recent data at this location, the oldest sea-level indicator (~7.5 cal kyr BP) is still not captured by any ice-earth model combination considered thus far. An alternative cause of this misfit is an inaccuracy in the eustatic component of the northern hemisphere model; this issue is explored below.

All of the regional melt models considered in this section perform badly at Larsemann and Vestfold. The fit at these sites was improved by the dominant Antarctic source scenario considered in Section 3.2, in which this region deglaciated at the time of mwp-IA. As for the case of the Ross Sea region, the cause of the over prediction of Holocene uplift in this region is ambiguous—it could be related to the timing of deglaciation (i.e. too late in the models considered in this section) or the magnitude of ice removal in the adopted model.

In Fig. 6, we conclude this analysis by revising the combined Ross/Weddell scenario to include a rapid deglaciation of the Lambert Glacier region (~0.15 m eustatic equivalent) at the time of mwp-IA as well as a northern hemisphere model in which the rate of melting dramatically reduces at 7 (rather than 6) cal kyr BP.

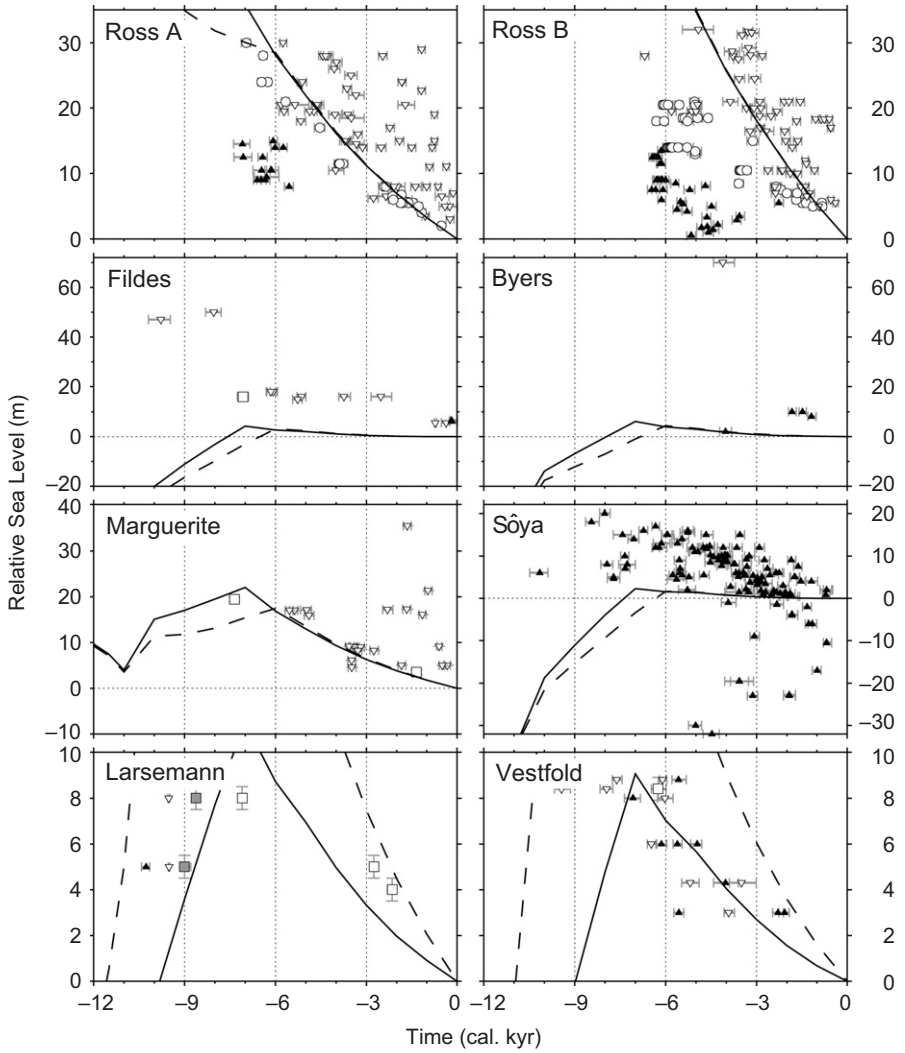

Fig. 6. Sea-level predictions based on the reference earth model and two different ice models. The dashed line shows the results for the combined (Ross/Weddell) model (solid line in Fig. 5) and the solid line shows the results for a revision of this model that includes rapid deglaciation of the Lambert Glacier region (~0.15 m eustatic) at the time of mwp-IA as well as cessation of rapid northern hemisphere ice melting at 7 cal kyr BP (compared to 6 cal kyr BP in our standard ice model).

This shift to a slightly earlier cessation of rapid northern hemisphere melting is not inconsistent with far-field sea-level observations (e.g. Fleming et al., 1998). Of the ice models considered in this analysis, the predictions based on this model (Fig. 6; solid line) are the most consistent with the observations.

4. Discussion and summary

The above results indicate that the available sea-level data are unable to preclude the existence of a significant contribution from the Antarctic Ice Sheet to mwp-IA. Our conclusion from this preliminary analysis is that, for the case of a dominant Antarctic source, most of the melt water was derived from the Weddell Sea (9 m) and the Ross Sea (5 m). This result is clearly not compatible with the field evidence that suggests the Ross Sea component of the ice sheet made a contribution of less than 1 m to mwp-IA (e.g. Licht, 2004). The total excess ice mass in the Ross Sea region of the adopted ice model is 10 m equivalent (eustatic) sea-level rise. The "best fit" model described above includes a 50% contribution from this region during mwp-IA with the remaining 50% being melted in a more gradual fashion until the mid-Holocene.

In the dominant North American source model considered in Fig. 3 (dashed line), there is a rapid deglaciation of the Ross Sea region between 10 and 8 cal kyr BP (this rapid change is a feature of the adopted ice model), which results in a poorer fit to the observations compared to the best fit model. The fit to the Ross Sea data may also be improved by reducing the magnitude of ice volume in this region (e.g. Bentley, 1999; Nakada et al., 2000; Licht, 2004). More modelling work is clearly required to investigate the sea-level response of a larger suite of Ross Sea deglaciation scenarios to determine which are consistent with the sea-level observations. Such an in-depth study of this region is beyond the scope of the present analysis.

Regardless of the ice or earth model adopted, there remain significant misfits to the observations from the South Shetland Islands and the Sôya coast. These discrepancies indicate that the adopted ice model, which has not been calibrated to fit any sea-level data, contains insufficient ice melt in these regions. These results are consistent with those of Nakada et al. (2000), who found that the ice models they considered also under-predicted the isostatic component of the sea-level response in the Sôya Coast and Antarctic Peninsula regions. The requirement of the observations for more extensive ice in the East Antarctic and the Peninsula clearly needs further exploration.

The relatively poor spatial extent of the data, the limited number of actual index points, and the lack of any constraints on sea-level prior to ~12 cal kyr BP imply that there are likely a number of possible ice melt scenarios that could provide adequate fits to the data. Our primary aim was to test whether the available data rule out a dominant Antarctic contribution to mwp-IA, and so the issue of non-uniqueness was not explored in any depth. Our analysis considered a small number of Antarctic deglaciation models that were derived from a single run of a glaciological model and so is clearly limited in this respect. The recent Antarctic deglaciation model proposed by Ivins and James (2005), which is based on field constraints and does not include an Antarctic component to mwp-IA, represents a useful alternative model that should be tested against the available sea-level observations.

The non-uniqueness problem can clearly be improved by obtaining, or improving, data from regions that are in proximity to the most likely mwp-IA source areas. For example, new observations obtained from, or closer to, the Weddell Sea region would help better constrain the Weddell Sea contribution to mwp-IA. Our results indicate that sea-level observations prior to ~8 cal kyr BP from Marguerite Bay would provide powerful constraints with which to test deglaciation models of the Weddell Sea and Peninsula regions.

This study has provided useful insight into the plausibility of an Antarctic source for mwp-IA. By exploring a number of melt scenarios based on a glaciologically realistic Antarctic ice model with a modified chronology, we have found that the data do not rule out a dominant Antarctic contribution to mwp-IA. Our preliminary analysis indicates that the Weddell Sea region is the most likely source for a large Antarctic contribution to mwp-IA. The Ross Sea is also plausible as a significant contributor from a sea-level perspective, although the geological field evidence can be used to argue against this. Our results also show that the adopted ice model under-predicts the isostatic component of the sea-level response in the Antarctic Peninsula and the Sôya Coast region of the East Antarctic ice sheet. It is plausible that ice melt from regions such as these, the Antarctic Peninsula in particular, could have made a significant contribution to mwp-IA.

Acknowledgments

We thank Peter Clark and Bert Vermeersen for constructive reviews of the original manuscript. SEB acknowledges the financial support of the Natural Environment Research Council of the UK. This paper is a contribution to IGCP Project 495 "Quaternary Land-Ocean Interactions" and the INQUA working group on "Coastal and Marine Processes".

References

Anderson, J.B., Shipp, S.S., Lowe, A.L., Wellner, J.S., Mosola, A.B., 2002. The Antarctic ice sheet during the last glacial maximum and its subsequent retreat history: a review. Quaternary Science Reviews 21, 49–70.

Baroni, C., Hall, B.L., 2004. A new Holocene relative sea-level curve for Terra Nova Bay, Victoria Land, Antarctica. Journal of Quaternary Science 19, 377–396.

Bassett, S.E., Milne, G.A., Mitrovica, J.X., Clark, P.U., 2005. Ice sheet and solid earth influences on far-field sea-level histories. Science 309, 925–928.

Bentley, M.J., 1999. Volume of Antarctic ice at the last glacial maximum, and its impact on global sea level change. Quaternary Science Reviews 18, 1569–1595.

Bentley, M.J., Anderson, J.B., 1998. Glacial and marine geological evidence for the ice sheet configuration in the Weddell Sea Antarctic Peninsula region during the last glacial maximum. Antarctic Science 10, 309–325.

Bentley, M.J., Hodgson, D.A., Smith, J.A., Cox, N.J., 2005. Relative sea level curves for the South Shetlands and Marguerite Bay regions, Antarctic Peninsula. Quaternary Science Reviews 24, 1203–1216.

Berkman, P.A., Forman, S.L., 1996. Pre-bomb radiocarbon and the reservoir correction for calcareous marine species in the Southern Ocean. Geophysical Research Letters 23, 363–366.

Clark, P.U., Alley, R.B., Keigwin, L.D., Licciardi, L.D., Johnsen, J.M., Wang, S.J., 1996. Origin of the first global meltwater pulse following the last glacial maximum. Paleoceanography 11, 563–577.

Clark, P.U., Mitrovica, J.X., Milne, G.A., Tamisiea, M.E., 2002. Sea level fingerprinting as a direct test for the source of global meltwater pulse IA. Science 295, 2438–2441.

Colhoun, E.A., Mabin, M.C.G., Adamson, D.A., Kirk, R.M., 1992. Antarctic ice volume and the contributions to sea-level fall at 20,00 yr BP from raised beaches. Nature 358.

Conway, H., Hall, B.L., Denton, G.H., Gades, A.M., Waddington, E.D., 1999. Past and future grounding-line retreat of the West Antarctic ice sheet. Science 286, 280–283.

Denton, G.H., Hughes, T., 2002. Reconstructing the Antarctic ice sheet at the last glacial maximum. Quaternary Science Reviews 21, 193–202.

Dziewonski, A.M., Anderson, D.L., 1981. Preliminary reference earth model (PREM). Physics of the Earth and Planetary Interiors 25, 297–356.

Emslie, S.D., McDaniel, J.D., 2002. Ade'lie penguin diet and climate change during the middle to late Holocene in northern Marguerite Bay, Antarctic Peninsula. Polar Biology 25, 222–229.

Fairbanks, R.G., 1989. A 17,000 year glacio-eustatic sea-level record: influence of glacial melting rates on the Younger Dryas event and deep ocean circulation. Nature 342, 637–642.

Fleming, K., Johnston, P., Zwartz, D., Yokoyama, Y., Lambeck, K., Chappell, J., 1998. Refining the eustatic sea-level curve since the last glacial maximum using far- and intermediate-field sites. Earth and Planetary Science Letters 163, 327–342.

Forte, A.M., Mitrovica, J.X., 1996. A new inference of mantle viscosity based on a joint inversion of post-glacial rebound data and long-wavelength geoid anomalies. Geophysical Research Letters 23, 1147–1150.

Gordon, J.E., Harkness, D.D., 1992. Magnitude and geographic-variation of the radiocarbon content in Antarctic marine life—implications for reservoir corrections in radiocarbon dating. Quaternary Science Reviews 11, 697–708.

Hall, B.L., Denton, G.H., 1999. New relative sea-level curves for the southern Scott Coast, Antarctica: evidence for Holocene deglaciation of the western Ross Sea. Journal of Quaternary Science 14, 641–650.

Hall, B.L., Baroni, C., Denton, G.H., 2004. Holocene relative sea-level history of the Southern Victoria Land Coast, Antarctica. Global and Planetary Change 42, 241–263.

Hanebuth, T., Stattegger, K., Pieter, M., 2000. Rapid flooding of the Sunda shelf: a late-glacial sea-level record. Science 288, 1033–1035.

Hindmarsh, R. 〈http://www.antarctica.ac.uk/met/rcah/agdb/index.htm〉.

Hughen, K.A., Baillie, M.G.L., Bard, E., Bayliss, A., Beck, J.W., Bertrand, C.J.H., Blackwell, P.G., Buck, C.E., Burr, G.S., Cutler, K.B., Damon, P.E., Edwards, R.L., Fairbanks, R.G., Friedrich, M., Guilderson, T.P., Kromer, B., McCormac, F.G., Manning, S.W., Bronk Ramsey, C., Reimer, P.J., Reimer, R.W., Remmele, S., Southon, J.R., Stuiver, M., Talamo, S., Taylor, F.W., van der Plicht, J., Weyhenmeyer, C.E., 2004. Marine04 Marine radiocarbon age calibration, 26 - 0 ka BP. Radiocarbon 46, 1059–1086.

Huybrechts, P., 2002. Sea-level changes at the LGM from ice-dynamic reconstructions of the Greenland and Antarctic ice sheets during the glacial cycles. Quaternary Science Reviews 21, 203–231.

Ivins, E.R., James, T.S., 2005. Antarctic glacioisotasy: a new assessment. In: XXVIII SCAR Meeting, Bremen.

Kaufmann, G., 1997. The onset of Pleistocene glaciation in the Barents Sea: implications for glacial isostaic adjustment. Geophsical Journal International 131, 281–292.

Kirk, R.M., 1991. Raised beaches, late Quaternary sea-levels and deglacial sequences on the Victoria Land coast, Antarctica. In: Gillieson, D.S., Fitzsimons, S. (Eds.), Quaternary Research in Australian Antarctica: Future Directions. Australian Defense Force Academy, Canberra, pp. 85–105.

Lambeck, K., 1993. Glacial rebound of the British isles—II. A high resolution, high precision model. Geophysical Journal International 115, 960–990.

Lambeck, K., 1995. Constraints in the late Wiechselian ice sheet over the Barents Sea from observations of raised shorelines. Quaternary Science Reviews 14, 1–16.

Lambeck, K., Nakada, M., 1990. Late Pleistocene and Holocene sea-level change along the Australian coast. Palaeogeography Palaeoclimatology Palaeoecology 89, 143–176.

Lambeck, K., Johnston, P., Nakada, M., 1990. Holocene glacial rebound and sea-level change in NW Europe. Geophysical Journal International 103, 451–468.

Lambeck, K., Smither, C., Johnstin, P., 1998. Sea-level change, glacial rebound and mantle viscosity for northern Europe. Geophysical Journal International 134, 102–144.

Lambeck, K., Yokoyama, Y., Purcell, T., 2002. Into and out of the last glacial maximum: sea-level change during Oxygen Isotope Stages 3 and 2. Quaternary Science Reviews 21, 343–360.

Licht, K.L., 2004. The Ross Sea's contribution to eustatic sea-level during meltwater pulse IA. Sedimentary Geology 165, 343–353.

Manabe, S., Stouffer, R.J., 1997. Coupled ocean-atmosphere model response to freshwater input: comparison to Younger Dryas event. Paleoceanography 12, 321–336.

McManus, J.F., Francois, R., Gherardi, J.-M., Keigwin, L.D., Brown-Leger, S., 2004. Collapse and rapid resumption of Atlantic meridonial circulation linked to deglacial climate changes. Nature 428, 834–837.

Milne, G.A., 1998. Refining models of the glacial isostatic adjustment process. Unpublished Ph.D. Thesis, University of Toronto.

Milne, G.A., Mitrovica, J.X., Davis, J.L., 1999. Near-field hydro-isostasy: the implementation of a revised sea-level equation. Geophysical Journal International 139, 464–482.

Milne, G.A., Davis, J.L., Mitrovica, J.X., Scherneck, H.-G., Johansson, J.M., Vermeer, M., Koivula, H., 2001. Space-geodetic constraints on glacial adjustment in Fennoscandia. Science 291, 2381–2385.

Mitrovica, J.X., Forte, A.M., 1997. The radial profile of mantle viscosity: results from the joint inversion of convection and post-glacial rebound observables. Journal of Geophysical Research 102, 2751–2769.

Nakada, M., Lambeck, K., 1988. The melting history of the late Pleistocene Antarctic ice sheet. Nature 333, 36–40.

Nakada, M., Lambeck, K., 1989. Late Pleistocene and Holocene sea-level change in the Australian region and mantle rheology. Geophysical Journal International 96, 497–517.

Nakada, M., Kimura, R., Okuno, J., Moriwaki, K., Miura, H., Maemoku, H., 2000. Late Pleistoscene and Holocene melting history of the Antarctic ice sheet derived from sea-level observations. Marine Geology 167, 85–103.

Okuno, J., Nakada, M., 1999. Total volume and temporal variation of meltwater from the last glacial maximum inferred from sea-level observations at Barbados and Tahiti. Palaeogeography, Palaeoclimatology, Palaeoecology 146, 283–293.

Peltier, W.R., 1974. The impulse response of a Maxwell earth. Reviews of Geophysics and Space Physics 12, 649.

Peltier, W.R., 2002. On eustatic sea-level history: last glacial maximum to Holocene. Quaternary Science Reviews 21, 377–396.

Peltier, W.R., 2005. On the hemispheric origins of meltwater pulse 1a. Quaternary Science Reviews 24, 1655–1671.

Peltier, W.R., Shennan, I., Drummond, R., Horton, B., 2002. On the postglacial isostatic adjustment of the British Isles and the shallow viscoelastic structure of the earth. Geophsical Journal international 148, 443–475.

Reimer, P.J., Baillie, M.G.L., Bard, E., Bayliss, A., Beck, J.W., Bertrand, C.J.H., Blackwell, P.G., Buck, C.E., Burr, G.S., Cutler, K.B., Damon, P.E., Edwards, R.L., Fairbanks, R.G., Friedrich, M., Guilderson, T.P., Hogg, A.G., Hughen, K.A., Kromer, B., McCormac, F.G., Manning, S.W., Ramsey, C.B., Reimer, R.W., Remmele, S., Southon, J.R., Stuiver, M., Talamo, S., Taylor, F.W., van der Plicht, J., Weyhenmeyer, C.E., 2004. IntCal04 Terrestrial radiocarbon age calibration, 26 - 0 ka BP. Radiocarbon 46, 1029–1058.

Rohling, E.J., Marsh, R., Wells, N.C., Siddall, M., Edwards, N.R., 2004. Similar meltwater contributions to glacial sea level changes from Antarctic and northern ice sheets. Nature 430, 1016–1021.

Shennan, I., Peltier, W.R., Drummond, R., Horton, B., 2002. Global to local scale parameters determining relative sea-level changes and the post-glacial isostatic adjustment of Great Britain. Quaternary Science Reviews 21, 397–409.

Stuiver, M., Reimer, P.J., 1993. Extended 14C database and revised CALIB radiocarbon calibration program. Radiocarbon 35, 215–230.

Takada, M., Tanib, A., Miura, H., Moriwaki, K., Nagatomo, T., 2003. ESR dating of fossil shells in the Lützow-Holm Bay region, East Antarctica. Quaternary Science Reviews 22, 1323–1328.

Tushingham, A.M., Peltier, W.R., 1991. Ice-3 g—a new global-model of Late Pleistocene deglaciation based upon geophysical predictions of postglacial relative sea-level change. Journal of Geophysical Research—Solid Earth and Planets 96, 4497–4523.

Verleyen, E., Hodgson, D.A., Milne, G.A., Sabbe, K., Vyverman, W., 2005. Relative sea-level history from the Lambert glacier region, East Antarctica, and its relation to deglaciation and Holocene glacier readvance. Quaternary Research 63, 45–52.

Wassell, A., Håkansson, H., 1992. Diatoom strtigraphy in a lake on Horeshoe Island, Antarctica. Diatom Research 7, 157–194.

Weaver, A.J., Saenko, O.A., Clark, P.U., Mitrovica, J.X., 2003. Meltwater pulse 1A from Antarctica as a trigger of the bolling-allerod warm interval. Science 299, 1709–1713.

Zhang, Q., Peterson, J.A., 1984. A geomorphology and late Quaternary geology of the Vestfold Hills, Antarctica. ANARE 133.

Zwartz, D., Bird, M.I., Stone, J.O., Lambeck, K., 1998. Holocene sea-level change and ice sheet history in the Vestfold Hills, East Antarctica. Earth and Planetary Science Letters 155, 131–145.